Ultrasound Images Edge Detection using Anisotropic Diffusion in Canny Edge Detector Framework

HUM YAN CHAI [1], LAI KHIN WEE [1, 2], EKO SUPRIYANTO[1]
[1]Department of Clinical Science and Engineering
Faculty of Health Science and Biomedical Engineering
Universiti Teknologi Malaysia
UTM Skudai, 81310 Johor
MALAYSIA
[2]Faculty of Computer Science and Automation
Institute of Biomedical Engineering and Informatics
Technische Universität Ilmenau,
98684, Ilmenau
GERMANY
eko@utm.my kwlai2@live.utm.my ychum2@live.utm.my http://www.biomedical.utm.my

Abstract: - Conventional Canny edge detector can detect edges in image with additive noise effectively but not ultrasound image that are corrupted by multiplicative speckle noise which alleviates image resolution resulting in inaccurate characterization of object features. In this paper, we proposed to incorporate the modified SRAD into the Canny edge detector to replace the Gaussian blurring in the conventional Canny edge detector in order to suppress the multiplicative noise effectively while preserving the edge of the object in ultrasound image. The result shows that the proposed method can provide better result than conventional method in a much wider range of parameter values. The proposed method through experimental result indicates that it is capable of producing promising edge detection result in ultrasound image.

Key-Words: - edge detection, speckle reducing anisotropic diffusion, ultrasound image enhancement, noise filtering

1 Introduction

Edge detection is defined as a process to identify the sharp discontinuities in an image. The discontinuities are often known as abrupt changes in pixel intensity or the pixels that characterize the boundaries of objects in an image. The edge detected contributes in many applications such as image segmentation[1-2], enhancement,[3], [34-38] compression and etc. The edge detection in digital image processing is always implemented by convolving the image with a 2D filter operator. The 2D filter is designed to be of high sensitivity towards large gradients in the image and return null values on pixels in homogenous region of image. Edge detection is a significant issue in image processing and pattern recognition. It is due to its ability to give the outline of an object, to supply information of the boundary between an object and background, to indicate overlapping objects, to calculate the basic properties of the object like area and shape[4-5] and to classify and identify essential information in image. The desired effect of any edge detection operation is giving no response to non-edge pixels and giving only one response to a single edge.

Different types of edges need to be detected using different design of the detector. Among the factors[6] that affect the design is the edge orientation, type of noise and the structure of the edge. The edge orientation [7-8] is important in determining a most sensitive characteristic direction like horizontal and vertical direction. Noises and edge both contain high-frequency content and thus difficult to detect edge in noisy image [9-10], attempts to diminish noises lead to blurred and distorted edges. Operator that detects edge in noisy environment is normally large in size in order to average the data to reduce the effect of noisy pixels. This results in inaccurate detection of desired edges. Not necessary that edges in image comprises of step change in pixel intensity, some boundaries[11] change intensity gradually, Therefore, an edge detection operator need to be designed to be designed to detect such edges[12]. Wavelet-based[13] technique is able to distinguish different type of edges.

Multitude algorithms of edge detection have been proposed. Among the common edge detection methods are Sobel method[14], Roberts[15], Prewitt[16]and Laplacian method[17], Rosenfeld and Thurston[18] and Marr- Hildreth[19]. These methods detect edges by utilizing masks to perform the convolution on the digital image according to the sudden change of gray level pixel intensity. Canny[20] make a modification on Sobel method. Canny searches the edge direction by inspecting the vertical and horizontal edge pixel intensity and implement non-maximum suppression to sharpen the edge. Among the earliest method, canny is the edge detector that can provide good edge detection performance in terms of single response to edge and good localization.

The conventional canny edge detector implements Gaussian blurring[8, 21-23] as the first step to reduce the effect of the noise during edge detection. This blurring effect at the same time leads to loss of important feature in the image especially the edge of the object. This issue has been observed by Perona and Malik[24] and they proposed a method, namely nonlinear anisotropic diffusion. This method is capable of blurring of noises and preserving of edges simultaneously. The smoothing effect is non-linear at different region in the image; Homogeneous region will have higher smoothing effect whereas region near edge will have lower smoothing effect. In other words, the algorithm encourages intra-region smoothing and alleviates inter-region smoothing. Besides protecting the edges of the object, the algorithm can even enhance the edge of the object by manipulating the diffusion direction; the diffusion parallel with edge will be higher compare to the diffusion across the edge.

The method has solved the problem of blurring of edge during smoothing process in image. However, it is not without limitation. Anisotropic diffusion[25-28] is only suitable in filtering of additive noise but not multicative noise. Ultrasound image adherently contains multicative noise and thus need an enhanced version of anisotropic diffusion to cope with the noise. Hence, Acton et al. [29] proposed speckle reducing anisotropic diffusion (SRAD) that capable of filtering the multicative noise. The strength of SRAD[30] is that it combines the statistical information of speckle noise into the anisotropic diffusion framework to smooth homogenous speckle regions while preserving image features.

The remainder of this paper is organized as follows: In section methodology, a series of proposed edge detection step combined with SRAD is discussed. In section result, experiments using the proposed algorithm on ultrasound phantom image will be set up and an elucidation about the result will be included. Next, there is a quantitative analysis on previous method.Finally, conclusions and future directions for edge detection in ultrasound are discussed.

2 Methodology

The methods that we proposed are the incorporation of SRAD in eight directions in Canny edge detector. The equation[31] in the continuous domain version based on a nonlinear partial differential model as following:

$$\frac{\partial I(x,y;t)}{\partial t} = div[c(q)\nabla I(x,y;t)] \tag{1}$$

Where (x,y) are image coordinates, t is diffusion time, $I(x,y;t)$ is the image intensity function, and $c(q) \in [0,1]$ is the diffusion coefficient. This PDE is typically discretezed by computing finite differences in for four directions at each image pixel. Modification has been done on the standard SRAD algorithm in this paper to increase the neighborhoods during discrete SRAD computations

The SRAD diffusion coefficient incorporates local speckle statistics and is defined as following:

$$c(q) = \frac{1}{1 + \dfrac{q^2(x,y;t) - q_o^2(t)}{q_o^2(t)(1+q_o^2(t))}} \tag{2}$$

$q(x,y)$, the instantaneous coefficient of variation (ICOV) is defined as following:

$$q(x,y;t) = \sqrt{\frac{(1/2)(|\nabla I / I|)^2 - (1/4)(\nabla^2 I / I)^2}{[1+(1/4)(\nabla^2 I / I)]^2}} \tag{3}$$

$q_o(t)$, the speckle scale function is defined as following:

$$q_o(t) = \frac{\sqrt{\mathrm{var}[z(t)]}}{\overline{z(t)}} \tag{4}$$

Where $\mathrm{var}[z(t)]$ represent variance and $\overline{z(t)}$ represents mean in a homogeneous region of fully developed speckle, z(t).

The pixels that contain ICOV that similar to speckle scale function are considered as homogenous region. Therefore the SRAD diffusion coefficient at the homogenous will equals to unity and thus will be smoothed. Similarly, the pixels near the edges will have higher value of ICOV and thus lead to a diffusion coefficient close to zero.

The image is anisotropic diffused with the following algorithm using 2D discrete implementation:

$$\frac{\partial}{\partial t}I(x,y,t) = div[g(x,y,t) * \nabla I(x,y,t)]$$
$$= \frac{\partial}{\partial x}[g(x,y,t) * \frac{\partial}{\partial x}I(x,y,t)] + \frac{\partial}{\partial y}[g(x,y,t).\frac{\partial}{\partial y}I(x,y,t)]$$

$$= \frac{1}{(\Delta x)^2}[g\left(x+\frac{\Delta x}{2},y,t\right).\left(I(x+\Delta x,y,t) - I(x,y,t)\right) + g\left(x-\frac{\Delta x}{2},y,t\right).(I(x-\Delta x,y,t) - I(x,y,t)] + \frac{1}{(\Delta y)^2}[g\left(x,y+\frac{\Delta y}{2},t\right).\left(I(x,y+\Delta y,t) - I(x,y,t)\right) + g\left(x,y-\frac{\Delta y}{2},t\right).(I(x,y-\Delta y,t) - I(x,y,t)] + \frac{1}{(\Delta d)^2}[g\left(x+\frac{\Delta x}{2},y+\frac{\Delta y}{2},t\right).\left(I(x+\Delta x,y+\Delta y,t) - I(x,y,t)\right) + g\left(x-\frac{\Delta x}{2},y-\frac{\Delta y}{2},t\right).(I(x-\Delta x,y-\Delta y,t) - I(x,y,t)] + \frac{1}{(\Delta d)^2}[g\left(x+\frac{\Delta x}{2},y-\frac{\Delta y}{2},t\right).\left(I(x+\Delta x,y-\Delta y,t) - I(x,y,t)\right) + g\left(x-\frac{\Delta x}{2},y+\frac{\Delta y}{2},t\right).(I(x-\Delta x,y+\Delta y,t) - I(x,y,t)]$$

$$= \Phi_{east} + \Phi_{west} + \Phi_{north} + \Phi_{south} + \Phi_{eastnorth} + \Phi_{westsouth} + \Phi_{westnorth} + \Phi_{eastsouth} \quad (5)$$

For the relative distance, Δx=Δy=1, Δd=$\sqrt{2}$.

The anisotropic diffusion filtering entails iterative update on each pixel in the image by the flow intensity contributed by its eight neighboring pixels:

$$\frac{\partial}{\partial t}\mathrm{I(x,y,t+\Delta t)} \approx \mathrm{I(x,y,t)} + \Delta t.[\Phi_{east} + \Phi_{west} + \Phi_{north} + \Phi_{south} + \frac{1}{(\Delta d)^2}(\Phi_{eastnorth} + \Phi_{westsouth} + \Phi_{westnorth} + \Phi_{eastsouth})]$$

$$= \mathrm{I(x,y,t)} + \Delta t.[\Phi_{east} + \Phi_{west} + \Phi_{north} + \Phi_{south} + \frac{1}{2}(\Phi_{eastnorth} + \Phi_{westsouth} + \Phi_{westnorth} + \Phi_{eastsouth})] \quad (6)$$

The purpose to smooth the image in canny detector is to reduce noise within an image. The filter used in Canny detector is a Gaussian low-pass filter. In this paper, we have replaced the Gaussian filtering with SRAD. After smoothing the image while preserving the feature edges, the next step is to compute the gradients. The magnitude of gradients is equals to strength of the edge while direction indicates the direction of the pixel that contains the highest grayscale change of intensity. The gradient is computed by convolution of the sobel kernel on each of the image pixel in x-direction and y-direction as following.

$$Kernel_x = \begin{bmatrix} -1 & 0 & 1 \\ -2 & 0 & 2 \\ -1 & 0 & 1 \end{bmatrix} \quad Kernel_y = \begin{bmatrix} 1 & 2 & 1 \\ 0 & 0 & 0 \\ -1 & -2 & -1 \end{bmatrix}$$

The magnitude, $|G|$ and directions θ are computed as following:

$$|G| = \sqrt{G_x^2 + G_y^2} \quad (7)$$

$$\theta = \tan^{-1}(\frac{G_y}{G_x}) \quad (8)$$

After obtaining the magnitude and direction of gradient, the next step is to sharpen the edge. To achieve this purpose, a series of steps need to be taken. Firstly, the gradient direction is rounded to nearest 45 degree. Next, make a comparison between the current pixel edge strength with the pixels in the positive and negative direction, only the pixel with maximum edge strength will be preserved, otherwise, it will be suppressed. The process mentioned is non-maximum suppression.

After the sharpening step, next to do is the reduction in edge numbers. Not all edges found in previous step are strong edges or true edges due to noises. Therefore, thresholding step is needed to distinguish strong edges from weak edges. First of all, two thresholds will be set, upper threshold and lower threshold. Pixels that contain gradients that higher than upper threshold will be preserved, whereas pixels that contain gradients lower then lower threshold will be suppressed. For pixels contain gradient between upper threshold and lower threshold, they will be called as weak edges and

only some of them will be chosen to stay in the last step. The process to select potential edges by setting two thresholds is called double thresholding.

The last step in the edge detection of canny edge detection involve suppressing all edges that are not connected to strong or true edges. The weak edges found in previous step can only be preserved to the final edge image if they are connected to the true edges. The reason for this step is to remove the weak edges that are caused by noises or other small variations. This process of selecting true edges from weak edges is named as hysteresis. The steps started from SRAD until hysteresis is summarized in the following flow chart.

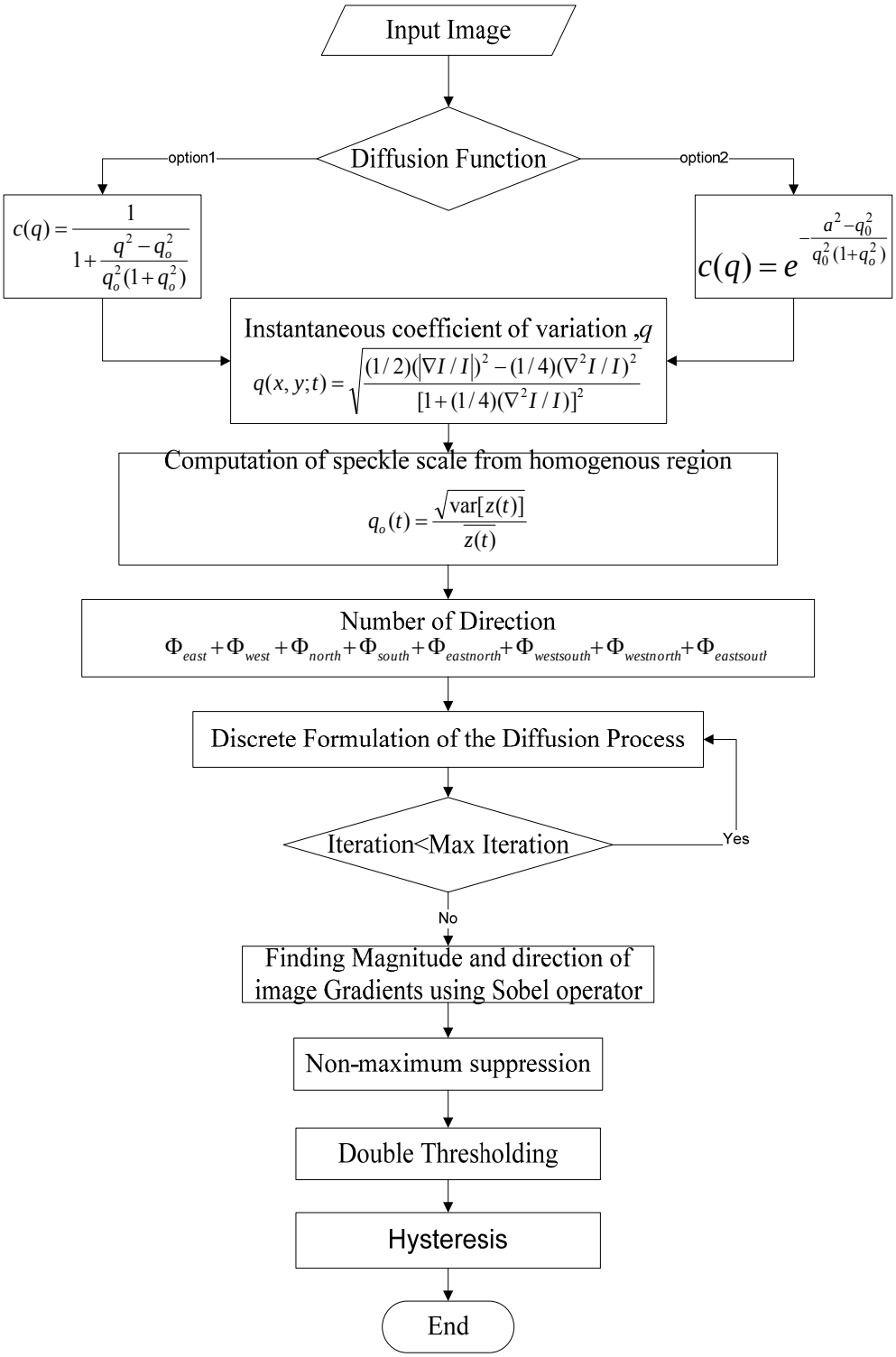

Fig.1 Flow chart of the methodology for the proposed edge detection

3 Results

In this section, the ultrasound phantom in figure 2.0 will undergo conventional canny edge detection and the proposed method edge detection at different thresholds and different standard deviation separately and the result is shown in figure 3.0 and figure 4.0.

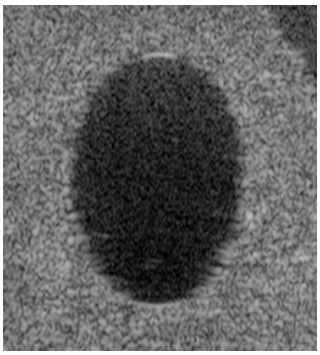

Fig. 2 Original ultrasound phantoms Image

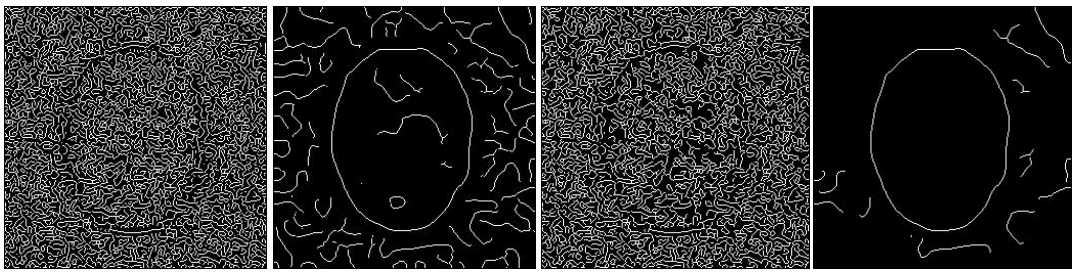

(a)Threshold=0.04,0.1 (b) Threshold=0.08,0.2

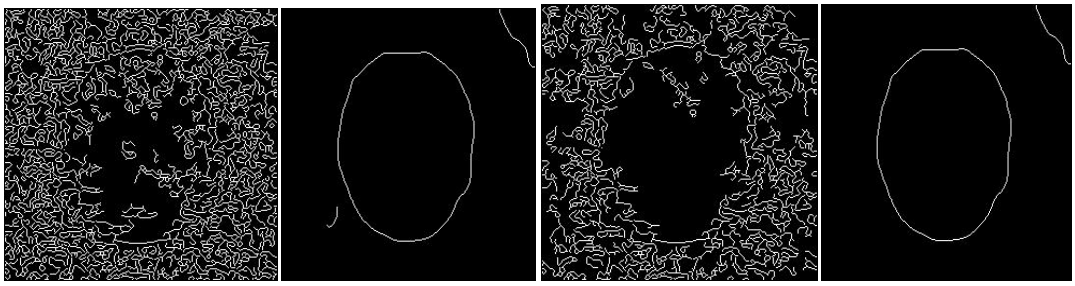

(c)Threshold=0.12,0.3 (d) Threshold=0.16,0.4

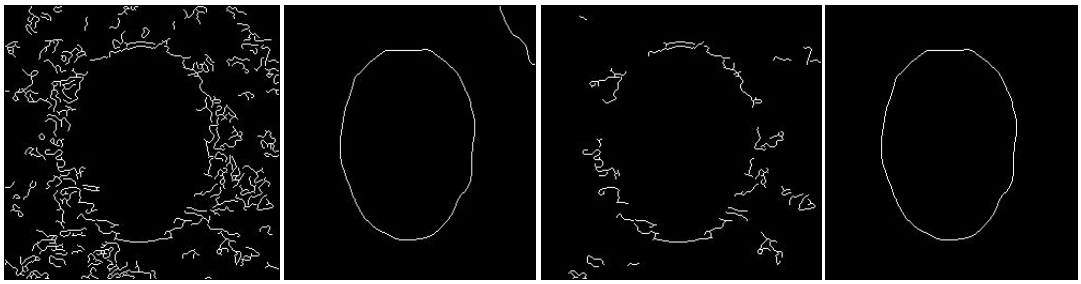

(e) Threshold=0.20,0.5 (f) Threshold=0.24,0.6

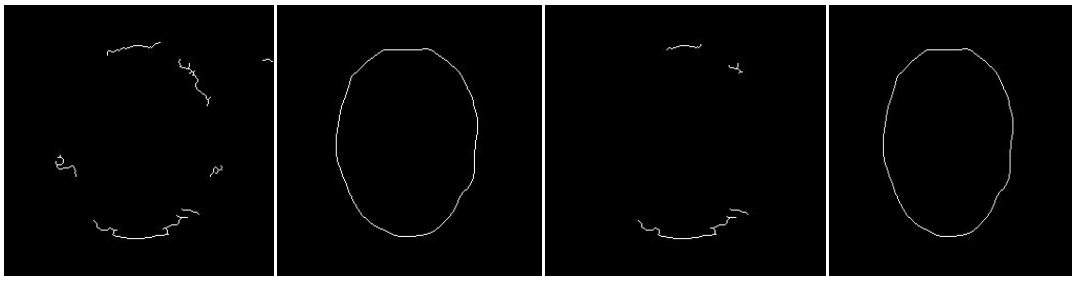

(g) Threshold=0.28,0.7 (h)Threshold=0.32,0.8

Fig. 3 Comparison between conventional canny edge detector and SRAD-Canny edge detector on noisy image of ultrasound with standard deviation of 1.0. The first and third columns are the image result by conventional canny detector. The second and fourth columns are the SRAD-Canny edge detector result image.

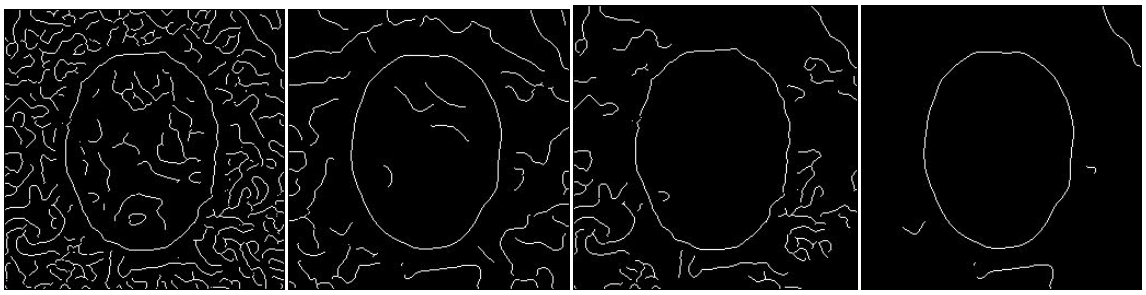

(a) Threshold=0.04,0.1 (b) Threshold=0.08,0.2

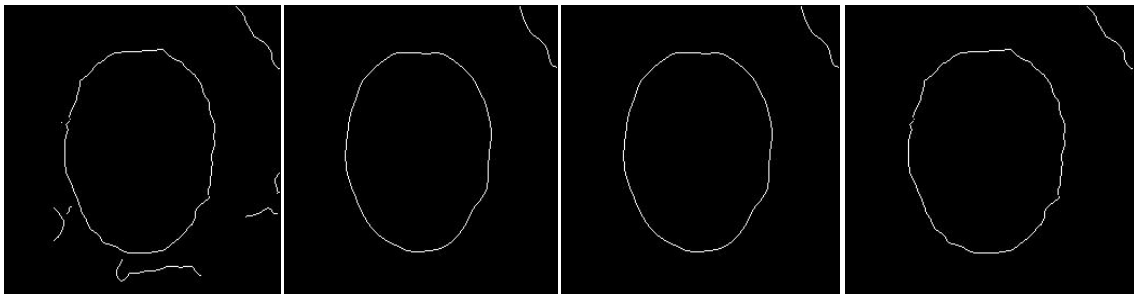

(c) Threshold=0.12,0.3 (d) Threshold=0.16,0.4

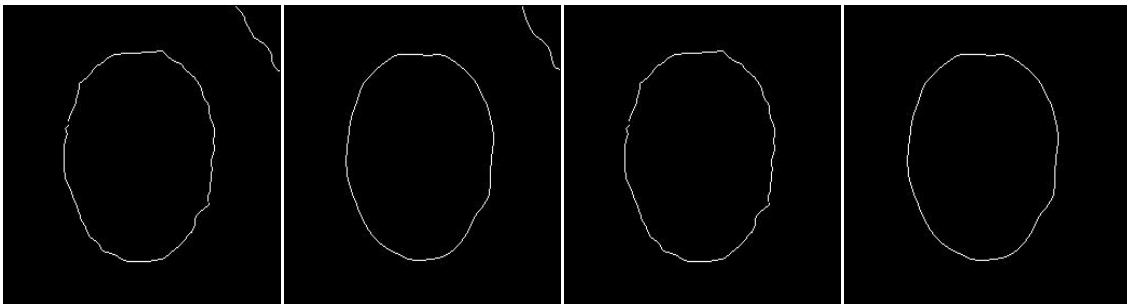

(e) Threshold=0.2,0.5 (f) Threshold=0.24,0.6

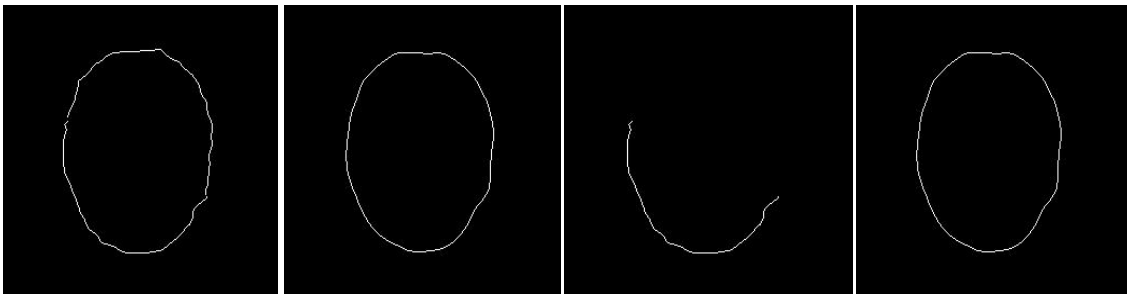

(g) Threshold=0.28,0.7 (h) Threshold=0.32,0.8

Fig. 4 Comparison between conventional canny edge detector and SRAD-Canny edge detector on noisy image of ultrasound with standard deviation of 3.0. The first and third columns are the image result by conventional canny detector. The second and fourth columns are the SRAD-Canny edge detector result image

4 Discussion

From figure 1, it can be observed that at threshold value of 0.1, the image generated from conventionally canny using Gaussian blurring result in a noisy result whereas the image generated using SRAD-Canny Edge detector shows less noisy result with the elliptical shape object observable. At threshold value of 0.2, 0.3 and 0.4, the conventional canny detector result remains a noisy image although the middle of the elliptical shape begin to appear whereas the SRAD-canny edge result in a clear and clean edge of the elliptic shape. At threshold 0.5, 0.6, 0.7, 0.8, the conventional canny detector result in less noisy edge around elliptic shape, however the strong edge of the elliptic shape is reduced as well, and the shape is not observable whereas the SRAD-canny is obviously presenting a complete shape of ellipse and free of noisy edges.

From figure 2, the edge detection is carried out in higher value of standard deviation of Gaussian blurring, at threshold of 0.1, 0.2, 0.3, the result image of conventional canny edge detector contains more noisy edges than SRAD-canny edge detector. At threshold of 0.4, 0.5, 0.6, 0.7, the elliptic shape is obtained for conventional canny edge, however, the shape is not complete, it can be found that small hole appears inside the shape. At higher value of threshold, the shape disappears and left a fraction of the edge. Through subjective evaluation, result shows that the conventional method is only capable of producing promising result if the parameter is correctly set. The proposed method, in contrast, can produce promising result in a very wider range of parameter values.

4.1 Quantitative analysis on the result

$$PSNR = 10\log_{10}\left(\frac{G_{\max}^2}{\sum_i^M \sum_j^N (I(i,j) - I^*(i,j))^2}\right) \tag{9}$$

Denotation: Where $G_{\max}$ is the maximum gray level of the image. where $I^*(i,j)$ represents pixel intensity in ith row and jth column processed image and $I(i,j)$ represents pixel intensity in ith row and jth column in the original image. M and N depicts maximum number of row and maximum number of column of the image matrix.

$$SNR = 10\log_{10}\left(\frac{\sigma_I^2}{\sigma_{I-I^*}^2}\right) \tag{10}$$

Denotation: where σ^2 denotes the variance of the original image, $\sigma_{I-I^*}^2$ denotes the variance of the smoothed image. The performance of the smoothing algorithm increases with the SNR value.

$$RMSE = \sqrt{\frac{1}{MxN}\sum_{i=1}^M \sum_{j=1}^N (I^*(i,j) - I(i,j))^2} \tag{11}$$

Where $I^*(i,j)$ represents pixel intensity in ith row and jth column processed image and $I(i,j)$ represents pixel intensity in ith row and jth column in the original image. M and N depicts maximum number of row and maximum number of column of the image matrix.The value of RMSE indicates the

total difference of pixel intensity in processed image and original image. Therefore, with larger value of RMSE, it indicates poorer information preservation.

$$FOM = \frac{1}{MAX\{N_a, N_d\}} \sum_{i=1}^{N_a} \frac{1}{1 + d_i^2 e} \quad (12)$$

Where N_r denotes actual edge map points, N_d denotes the ideal edge map points. d is the Euclidean distance difference calculated as actual edge point normal to a line of ideal edge points. The e denotes weighting factor. The *FOM* is equals to unity if the actual edge is perfectly merged with the detected edge. The weighting factor can be adjusted to penalize edges that are localized but deviated from the ideal position.

The result shown in table 1 indicates that the proposed method can produce image that has highest value of PSNR, SNR and RMSE. This implies that the proposed method produce less pixilated image. Besides, the FOM value indicates that the proposed method can detect edge with higher accuracy. All the highest value in the table has been bold for the comparison sake.

Table 1 Performance comparisons for ultrasound phantom image using quantitative analysis

	Quantitative Evaluations			
	PSNR	SNR	RMSE	FOM
Gaussian	13.3253	8.4564	29.4356	0.1356
KUAN[32]	14.3245	8.8976	27.3546	0.2465
AWMF[33]	14.2132	9.4564	26.4337	0.4566
SRAD[29]	16.4654	10.5676	15.4674	0.6342
PMAD[24]	14.6768	9.5468	19.3445	0.5434
PROPOSED	**17.4546**	**12.3556**	**13.7344**	**0.6779**

5 Conclusion

This paper presented an improved Canny edge detector by incorporating it with Speckle reducing anisotropic diffusion method in eight directions which can adapt to ultrasonic local speckle statistic. Experimental results on ultrasound phantom shows that the proposed method can preserve edges and small structures while removing speckle noise effectively at a wide range of threshold and standard deviation. Thus, it has the potential to enhance the diagnostic ultrasound imaging and to improve automated segmentation and edge detection technique. Future efforts should be focus on the thresholding step in Canny edge detection in order to make it become more adaptive to the noisy image.

References:

[1] Tang, H., et al., MRI brain image segmentation by multi-resolution edge detection and region selection. *Computerized Medical Imaging and Graphics*, Vol. 24, No. 6, 2000, pp. 349-357.

[2] Chai, H.Y., et al., GLCM based adaptive crossed reconstructed (ACR) k-mean clustering hand bone segmentation, *in 10th WSEAS international conference on signal processing, robotics and automation.*, 2011 pp. 192-197.

[3] Sauer, K., Enhancement of low bit-rate coded images using edge detection and estimation. *CVGIP: Graphical Models and Image Processing*, Vol. 31, No. 1, 1991, pp. 52-62.

[4] Garlipp, T. and C.H. Müller, Detection of linear and circular shapes in image analysis. *Computational Statistics & Data Analysis*, Vol. 51, No. 3, 2006, pp. 1479-1490.

[5] Chai, H.Y., et al., Adaptive Crossed Reconstructed (ACR) K-mean Clustering Segmentation for Computer-aided Bone Age Assessment System. International Journal of *Mathematical Models and Methods in Applied Sciences*, Vol. 5, No.3, 2011, pp. 628-635.

[6] Román-Roldán, R., et al., A measure of quality for evaluating methods of segmentation and edge detection. *Pattern Recognition*, Vol.34, No.5, 2001, pp. 969-980.

[7] Yu, Y.-H. and C.-C. Chang, A new edge detection approach based on image context analysis. *Image and Vision Computing*, Vol. 24, No.10, 2006, pp. 1090-1102.

[8] Accame, M. and F.G.B. De Natale, Edge detection by point classification of Canny

filtered images. *Signal Processing*, Vol.60, No.1, 1997, pp. 11-22.
[9] Johnson, R.P., Contrast based edge detection. *Pattern Recognition*, Vol.23, No.3, 1990, pp. 311-318.
[10] Chai, H.Y., et al., Gray-level co-occurrence matrix bone fracture detection. *American Journal of Applied Sciences*, Vol.8, No.1, 2011, pp. 26-32.
[11] Clark, J.J., Authenticating edges produced by zero-crossing algorithms. *Pattern Analysis and Machine Intelligence, IEEE Transactions on*, Vol.11, No.1, 1989, pp. 43-57.
[12] Aarnink, R., et al., Edge detection in prostatic ultrasound images using integrated edge maps. *Ultrasonics*, Vol.36, No.1, 1998, pp. 635-642.
[13] Shih, M.-Y. and D.-C. Tseng, A wavelet-based multiresolution edge detection and tracking. *Image and Vision Computing*, Vol.23, No.4, 2005, pp. 441-451.
[14] Gonzalez, R. and R. Woods, Digital Image Processing: Addison-Wesley Longman Publishing Co., Inc., 2001
[15] Roberts, L., Machine perception of three-dimensional solids, Massachusetts Institute of Technology, 1963
[16] Chaudhuri, B.B. and B. Chanda, The equivalence of best plane fit gradient with Robert's, Prewitt's and Sobel's gradient for edge detection and a 4-neighbour gradient with useful properties. *Signal Processing*, Vol.6, No.2, 1984, pp. 143-151.
[17] Mlsna, P.A. and J.J. Rodriguez, Gradient and Laplacian Edge Detection, in Handbook of Image and Video Processing (Second Edition), B. Al, Editor. 2005, Academic Press: Burlington. pp. 535-553.
[18] Rosenfeld, A. and M. Thurston, Edge and Curve Detection for Visual Scene Analysis. *Computers, IEEE Transactions on,* Vol.20, No.5, 1971, pp. 562-569.
[19] Marr, D. and E. Hildreth, Theory of Edge Detection. Proceedings of the Royal Society of London. Series B, *Biological Sciences*, Vol.207, No.1167, 1980. pp. 187-217.
[20] Canny, J., A Computational Approach to Edge Detection. *Pattern Analysis and Machine Intelligence, IEEE Transactions on*, Vol.8, No.6, 1986, pp. 679-698.
[21] Heath, M.D., et al., A robust visual method for assessing the relative performance of edge-detection algorithms. *Pattern Analysis and Machine Intelligence, IEEE Transactions on*, Vol.19, No.12, 1997, pp. 1338-1359.
[22] Medina-Carnicer, R., et al., A novel method to look for the hysteresis thresholds for the Canny edge detector. *Pattern Recognition*, Vol.24, No.6, 2011. pp. 1201-1211.
[23] Hou, Z.J. and G.W. Wei, A new approach to edge detection. *Pattern Recognition*, Vol.35, No.7, 2002. pp. 1559-1570.
[24] Perona, P. and J. Malik, Scale-space and edge detection using anisotropic diffusion. *Pattern Analysis and Machine Intelligence, IEEE Transactions on*, Vol.12, No.7, 1990. pp. 629-639.
[25] Xiaona, Z. and W. Tianfu. An anisotropic diffusion filter for ultrasonic speckle reduction. in Visual Information Engineering, 2008. *VIE 2008. 5th International Conference on*. 2008.
[26] Byeongcheol, Y. and T. Nishimura. A study of ultrasound images enhancement using adaptive speckle reducing anisotropic diffusion. in Industrial Electronics, 2009. ISIE 2009. IEEE International Symposium on. 2009.
[27] Aksel, A., et al. Speckle Reducing Anisotropic Diffusion for Echocardiography. in Signals, Systems and Computers, 2006. ACSSC '06. Fortieth Asilomar Conference on. 2006.
[28] Yoo, B.C., et al. Multi-scale Based Adaptive SRAD for Ultrasound Images Enhancement. in World Congress on Engineering and Computer Science 2008, WCECS '08. Advances in Electrical and Electronics Engineering - IAENG Special Edition of the. 2008.
[29] Yongjian, Y. and S.T. Acton, Speckle reducing anisotropic diffusion. *Image Processing, IEEE Transactions on*, Vol.11, No.11, 2002. pp. 1260-1270.
[30] Liu, G., et al., Speckle reduction by adaptive window anisotropic diffusion. *Signal Processing*, Vol.89, No.11, 2009. pp. 2233-2243.
[31] Gerig, G., et al., Nonlinear anisotropic filtering of MRI data. *Medical Imaging, IEEE Transactions on*, Vol.11, No.2, 1992. pp. 221-232.
[32] Kuan, D., et al., Adaptive restoration of images with speckle. Acoustics, *Speech and Signal Processing, IEEE Transactions on*, Vol.35, No.3, 1987. pp. 373-383.
[33] Loupas, T., W.N. McDicken, and P.L. Allan, An adaptive weighted median filter for speckle suppression in medical ultrasonic images. *Circuits and Systems, IEEE Transactions on*, Vol.36, No.1, 1989. pp. 129-135.
[34] Lai Khin Wee, Hum Yan Chai, Eko Supriyanto, Surface rendering of three dimensional ultrasound images using VTK,

Journal of Scientific & Industrial Research, Vol. 70, 2011, pp. 421-426.

[35] Wee L.K., Eko S., Automatic Detection of Fetal Nasal Bone in 2 Dimensional Ultrasound Image Using Map Matching, *12th WSEAS International Conference on Automatic Control, Modeling & Simulation*, 2010, pp. 305-309.

[36] Eko S., Wee L.K., Min T.Y., Ultrasonic Marker Pattern Recognition and Measurement Using *Artificial Neural Network, 9th WSEAS International Conference on Signal Processing*, 2010, pp. 35-40.

[37] Wee L.K., Arroj A., Eko S., Computerized Automatic Nasal Bone Detection based on Ultrasound Fetal Images Using Cross Correlation Techniques, *WSEAS Transactions on Information Science and Applications*, Vol. 7, No. 8, 2010, pp. 1068-1077.

[38] Wee L.K., et al., Nuchal Translucency Marker Detection Based on Artificial Neural Network and Measurement via Bidirectional Iteration Forward Propagation, *WSEAS Transactions on Information Science and Applications*, Vol.7, No.8, pp. 1025-1036.